

Effect of agglomeration of carbon nanotubes on gas permeability of PVTMS/CNT mixed matrix membranes

A M Grekhov^{1,2}, Yu S Eremin¹, D Bakhtin² and V V Volkov^{1,2}

¹National Research Nuclear University MEPhI (Moscow Engineering Physics Institute),
Kashirskoe highway 31, Moscow, 115409, Russia

²A.V.Topchiev Institute of Petrochemical Synthesis, Russian Academy of Sciences, Russia

E-mail: yseremin@ya.ru

Abstract. Mixed matrix membranes (MMMs) with unique transport characteristics can be prepared by the addition of the minor amounts of carbon nanotubes. Qualitative (critical, effective, marked) changes in the membrane performance are shown to be provided by the formation of a percolation cluster composed of nanotubes. For MMMs based on poly(trimethylvinylsilane) (PVTMS) containing carbon nanotubes (CNT), due to the formation of the CNT percolation cluster, gas permeability increases by a factor of 5-15. When the CNT content in the MMMs is higher than the percolation threshold, gas permeability remains on the same level or even decreases. Numerical simulation proves that the above negative changes are provided by the agglomeration of nanotubes and subsequent deterioration of the percolation structure in the membranes.

1. Introduction

Polymer-based membranes are widely used in various industrial-scale membrane technologies to separate and purify gases and liquids [1, 2]. Despite the fact that non-organic membranes based on either zeolites or carbon materials have higher permeability and selective values, polymer-based membranes have better mechanical, strength and technological characteristics. Besides, recently, new polymer materials have been synthesized, of which transport characteristics are close to non-organic materials [4]. However, the synthesis of new polymers is quite a long process, therefore alternative methods for improving the transport properties of polymer membranes still remain urgent, for instance the development of “mixed matrix membranes” (MMM) that are polymers containing non-organic nanoparticles [22-28].

Particles embedded into MMM can be split into several types: non-porous particles (SiO₂, TiO₂, etc.), nanoporous particles (zeolites, porous earth silica, MOF) and nanoparticles with a high aspect number (carbon fiber and nanotubes). Carbon nanotubes (CNTs) have some specific features as compared to other particles that makes CNT-based membranes the most promising MMM samples. Firstly, high strength characteristics of CNTs increase greatly the membranes strength [29]. Secondly, a significant change in the CNT-based MMM permeability is observed at a concentration of nanotubes of less than 2% that is several times less than the target concentration of other particles. However, it appeared that at high CNT concentration, no further improvement on the MMM transport properties is



observed but some worsening in the membranes parameters. For instance, the permeability of gases (He, H₂, CO₂, O₂, N₂, CH₄) through polydimethylsiloxane-based membranes increases as 2% of CNTs is embedded and changes insignificantly as the CNT concentration increases up to 10%. [2]. The same phenomenon is observed as the CNT concentration increases from 2 to 10%wt in PES-based membranes; the permeability of N₂ and CO₂ increases insignificantly, while the selectivity decreases [9]. The pervaporation permeability of the mixture water/ethanol (10/90) through hydrophilic polymer PVA increases monotonously as 1-5%wt of CNTs is embedded [10], however, the membrane selectivity decreases significantly when the CNT concentration is more than 3%. The minimal permeability and the maximal selectivity are observed at a CNT concentration of 2%wt in PVA during the water/isopropanol (20/80) mixture pervaporation as the CNT concentration increases from 2 to 4%wt [30]. The maximal change in the permeability was observed for some polymers as the CNT concentration raised. Such changes were observed for MMM with CNTs based on poly 2,6-dimethyl-1,4phenylene oxide [31], polysulphone [32], polyimidesiloxane [2]. This non-linear change in the permeability with the CNT concentration increase can not be explained by the traditional models, where the change of membrane properties is in proportion to the concentration of embedded nanoparticles. Some non-linear effects, for instance the permeability threshold change, can be explained by the percolation theory [2], polysulphone [32].

At a low CNT concentration, isolated areas of modified polymer of high permeability appear in the membrane and molecules successively go through the areas of high and low permeability. That is why the change in flow through the membrane is in proportion to the CNT concentration and, at low CNT concentration, it increases insignificantly. At a certain concentration, the embedded nanotubes generate a cluster that bounds two membrane surfaces. There appear an additional “parallel” flow through this cluster and the membrane permeability increases significantly that determines the threshold change in the permeability of MMM with embedded CNTs. However, to explain the non-linear changes in the permeability with further CNT concentration, one need to analyze the conditions of the percolation cluster formation and its structure. To explain the ultimate changes in the permeability, some papers give suppositions about the relation of the membrane permeability drop to the nanotubes agglomeration as the CNT concentration rises. The interaction between molecules and agglomerates causes an increase in the diffusion path tortuosity and decrease in the membrane permeability. However, according to the calculations, the nanotubes agglomeration also causes changes in the percolation cluster parameters that intensifies worsening in the membrane transport characteristics.

This paper presents the research in the permeability of membranes based on glassy polymer polyvinyltrimethylsilane PVTMS with embedded MWCNT and shows a percolation mechanism of permeability change at a CNT concentration of 0.45wt. However, at a concentration of more than 1%wt, the permeability remained the same; this phenomenon was explained by the numerical modeling of the transport characteristics of the CNT-based MMM with the account of nanotubes agglomeration and changes in the percolation cluster structure.

2. Experimental

2.1 Materials

In this work, we used the multiwalled carbon nanotubes (CNT) (TAUNITTM, NanoTekhCenter LLC, Russian Federation) prepared by chemical precipitation from a gaseous phase. According to technical specifications, TAUNITTM carbon nanomaterial is composed of fibrils based on polycrystalline graphite with a length below 2 microns; their outer diameter varied from 20 to 70 nm, specific surface was 120-130 m²/g, and the bulk density was 0.4-0.6 g/cm³. After the treatment with nitric acid according to the standard procedure [12], density of the CNT samples was 2.26±0.03 g/cm³, specific volume was $V = 0.20 \pm 0.02$ cm³/g, and the surface area was $S = 150 \pm 5$ m²/g. The inner diameter of the nanotubes was calculated by the BJH method from the low-temperature nitrogen sorption data, and this value was 3-6 nm. For the model of cylindrical channels, the outer CNT diameter was 20-60 nm.

We used the commercial PVTMS sample with a density of 0.86 g/cm^3 : the permeability coefficients were $P(\text{H}_2) = 220$, $P(\text{O}_2) = 44$, $P(\text{CH}_4) = 13$ barrer [13].

2.2 Membranes

Mixed matrix membranes were prepared mixing PVTMS and CNT solutions in chloroform. Carbon nanotubes were dispersed in chloroform by the ultrasound treatment for 15 min. The dimensions of agglomerates and individual CNT units were estimated by the dynamic laser scattering measurements [14]. The dimensions of agglomerates in the solution fit the dimensions of individual nanotubes with a diameter varying from 20 to 70 nm and with a length from 1 to 2 μm . The chloroform solution of PVTMS (3 wt %) was prepared under normal conditions then and filtered. Concentrations of PVTMS and CNTs in the chloroform solutions were controlled by their optical density. The membranes were prepared by casting the PVTMS and CNT solutions on a cellophane support. Chloroform was evaporated under normal conditions (atmospheric pressure, $T = 20\text{--}24^\circ\text{C}$) until the constant weight was attained. Thickness of the prepared membranes was $25 \pm 2 \text{ }\mu\text{m}$. We prepared the PVTMS/CNT membranes containing 0.2, 0.4, 0.8, 1.2, 1.5, 2 and 3 wt % of CNTs; the error was below 0.1%. The content of CNTs in PVTMS was estimated by the helium pycnometry method.

2.3 Methods and Equipment

The density of CNTs, PVTMS, and the related mixed matrix membranes was measured using a Micro-Ultrapyc 1200e Quantachrome density helium pycnometer; their specific surface and volume of pores were estimated by the low-temperature nitrogen sorption (Nova 1200e, Quantachrome). The inner diameter of the CNT channels d_{in} was calculated according to the BJH method [15]; the specific surface was estimated according to the BET method [16].

Concentrations of PVTMS and CNT solutions in chloroform was controlled by their optical density using a Hach 500 DR Lange spectrophotometer; the accuracy was 0.01 abs. The integral absorption coefficient of PVTMS was measured in the 300–500 nm wavelength interval, thus making possible to control the PVTMS concentration with an accuracy of 0.2 wt %. The absorption coefficient of CNT was measured at a wavelength of 600 nm; the accuracy was not less than 0.05 wt %. The dimensions of CNTs in chloroform were studied by the dynamic laser scattering method (DLS) at a wavelength of 780 nm (Nanotracs 252, Microtrac Inc.).

Permeability of ethanol through the PVTMS/CNT membranes was measured by the dynamic pressure decay method [17], the initial excessive pressure gradient was 200 atm, and the temperature was 30°C . The membrane permeability was calculated from the pressure decay rate over a membrane:

$$P_l = \frac{\chi \cdot V \cdot \Delta p \cdot \rho}{\Delta t} \cdot \frac{d}{S \cdot p} \quad (1)$$

where p is the current pressure in the liquid [atm], Δp is the pressure decay within time Δt [s], V is the volume of the liquid over the membrane [m^3], χ is the fluid compressibility [atm^{-1}], ρ is the liquid density [kg/m^3], d and S stand for the membrane thickness [m] and membrane area [m^2], respectively.

Gas permeability of nitrogen, oxygen, methane, and propane through the PVTMS/CNT membranes were measured by the Дайнеса-Баррера Barrer method at a pressure gradient of 4 atm; the temperature was $19\text{--}24^\circ\text{C}$. The permeability coefficients were calculated as:

$$P_{gas} = \frac{V \cdot d}{S \cdot \Delta p \cdot \Delta t} \quad (2)$$

where Δt is the time period within which the pressure changes by Δp [atm], V is the reference volume [m^3], d is the membrane thickness [m], S is the membrane area [m^2].

3. Results and Discussion

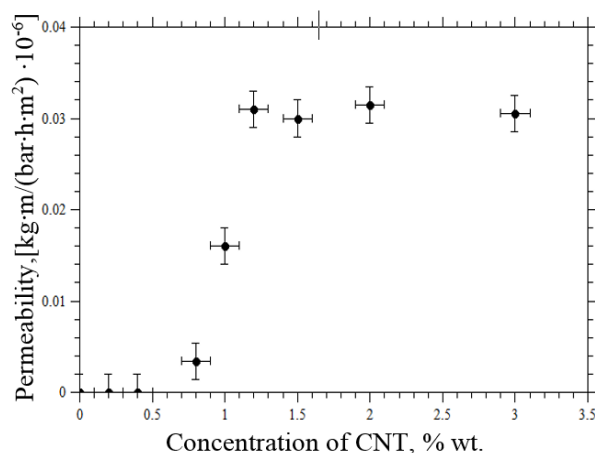


Figure 1. Permeability coefficient of ethanol for the PVTMS/CNT membranes.

Figure 1 presents the permeability coefficient of ethanol plotted against the CNT content in the PVTMS/CNT membranes and the plot shows three well-pronounced regions. When the CNT content in the PVTMS/CNT membranes is below 0.4 wt %, ethanol does not penetrate the mixed matrix membranes. The fact that the experimentally measured permeability of ethanol through the PVTMS-based membranes containing less than 0.4 wt % of CNT is absent means that the membrane does not have any regions which are permeable to ethanol. As the concentration of CNTs in the membrane is increased from 0.8 to 1.5 wt %, the permeability markedly increases by nearly a factor of 10. Hence, one can conclude that this increase in the ethanol permeability of the membrane takes place once a certain percolation CNT concentration is achieved and this concentration lies between 0.4 and 0.8 wt %. In this case, interconnected PVTMS/CNT regions are formed and these regions are permeable for ethanol. The number of these channels nonlinearly increases with increasing CNT concentration from 0.8 to 1.5 wt %. When the CNT content in the membrane is higher than 1.5 wt %, the growth in the membrane permeability is ceased. Noteworthy is that the gas permeability of the PVTMS/CNT membranes follows the same scenario.

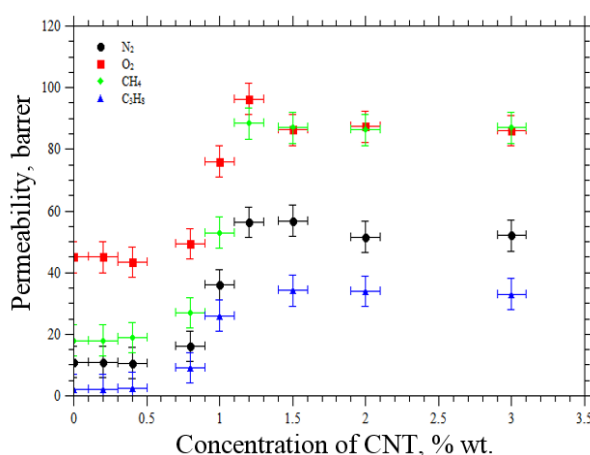


Figure 2. Gas permeability through the PVTMS/CNT membranes

Figure 2 presents the gas permeability of the PVTMS/CNT membranes for nitrogen, oxygen, methane, and propane plotted against the CNT concentration in the membrane, and this plot also shows three well-pronounced concentration intervals. When the CNT content in the membrane is lower than 0.4 wt %, gas permeability of the matrix mixed membranes for all gases under study is

equal to the permeability of the neat PVTMS. When the CNT content is changed from 0.8 to 1.5 wt %, gas permeability increases in the following manner: by a factor of 5 for nitrogen, by a factor of two for oxygen, 4 for methane, and 15 for propane. When the CNT content is higher than 1.5 wt %, the growth in the gas permeability is ceased and this value remains virtually constant. This increase in the gas permeability of the PVTMS/CNT membranes at the threshold CNT concentration has been reported earlier but the fact that, at the higher CNT content, the permeability becomes invariable is new [11]. This behavior was also observed for other glassy polymers. For example, gas permeability through the poly(dimethyl siloxane)-based membranes increases when the CNT content is equal to 2% but it remains virtually unchanged with increasing CNT concentration up to 10% [6]. For the polysulfone-based membranes, as the content of CNTs increases from 2 to 10 wt %, N₂ and CO₂ permeability slightly increases but selectivity is compromised [7].

This nonlinear change in the permeability of the mixed matrix membranes suggests that permeability of the mixed matrix membranes is controlled by the parameters of the formed percolation cluster. Traditionally, when two different materials are mixed, any additive changes in their characteristics can be described by the mixture rule. For example, as follows from Fig. 3, the density of the PVTMS/CNT membranes changes linearly and can be described by the following equation $\rho_{MMM} = c_{CNT} \cdot \rho_{CNT} + (1 - c_{CNT}) \cdot \rho_{PVTMS}$. Here, ρ_{MMM} is the density of the mixed matrix membranes, ρ_{CNT} is the density of CNTs (2.267 g/cm³), c_{CNT} is the weight content of CNTs in the PVTMS/CNT membranes, ρ_{PVTMS} is the density of PVTMS (0.9135 g/cm³).

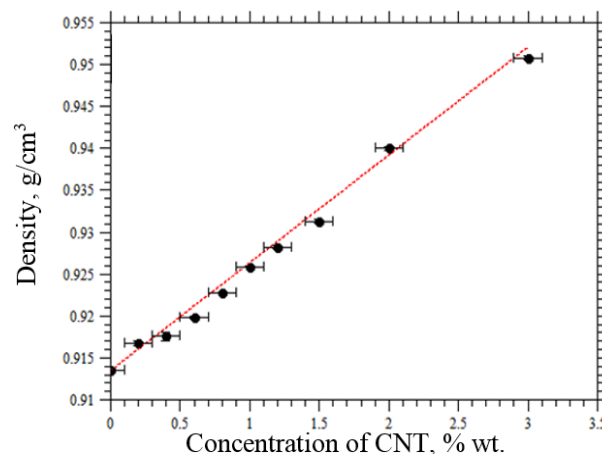


Figure 3. Density of the hybrid PVTMS/CNT membranes

By analogy, if permeability of the mixed matrix membranes depends on the content of nanotubes, this parameter can be described by the following relationship: $P_{MMM} = P_{CNT} \cdot c_{CNT} + P_{PVTMS} \cdot (1 - c_{CNT})$, where P_{CNT} is the permeability of the membrane regions containing CNTs and P_{PVTMS} is the permeability of the CNT-free PVTMS. In this case, permeability of the ideal mixed matrix membranes should change linearly with increasing CNT concentration. However, this approach fails to describe the experimentally observed changes in the permeability of the mixed matrix PVTMS/CNT membranes. If changes in the net membrane permeability are provided by the development of highly permeable open channels in the membrane, permeability starts to increase only when CNTs are organized into the percolation cluster; in this case, permeability should be proportional to the volume of the percolation cluster:

$$P_{MMM} = P_{\infty} \cdot x_{\infty} + P_{PVTMS} \cdot (1 - x_{\infty}) \quad (3)$$

where x_{∞} is the volume fraction of the membrane occupied by the percolation cluster, P_{∞} is the permeability coefficient of the percolation cluster, P_{PVTMS} is the permeability coefficient of PVTMS. Changes in the membrane permeability and x_{∞} are nonlinear when concentration of nanotubes in the

membrane is above the percolation threshold. At low CNT concentrations, the percolation cluster does not exist or, in other words, x_∞ is equal to zero and the presence of nanotubes has no effect on the membrane permeability.

The effect of the percolation cluster on the permeability of the mixed matrix membranes was studied according to the Monte Carlo scheme which allows one to assess the conditions providing the formation of the percolation structures composed of nanotubes in the 3D space and their characteristics. We used the standard algorithms such as the Mersenne twister for the estimation of coordinates and orientation of CNTs [18], the Hashen-Koppelman algorithm for the calculation of the CNT distribution over the clusters [19], and the method of the percolation cluster detection [20, 21].

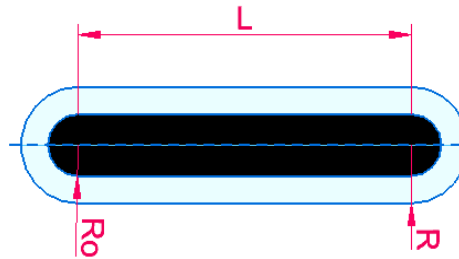


Figure 4. The model of a carbon nanotube as a capsule with an impermeable core and a permeable shell.

In the simulation experiments, nanotubes (which are modeled as capsules with a diameter varying from 0.05 to 0.08 units and with a length of 2 units) are randomly distributed on a $25 \times 25 \times 25$ matrix. Both diameter (0.05) and length (2 units) are proportional to the dimensions of CNTs used in our experiments (the CNT diameter is 50 nm and the CNT length is 2 μm); the bigger capsules correspond to the agglomerates of nanotubes. Volume concentration of nanotubes or, in other words, the volume occupied by the capsules reads as: $x = \left(\frac{4\pi}{3} \cdot R_0^3 + \pi \cdot R_0^2 \cdot L \right) \cdot N/V$, where R_0 is the radius of the impermeable core, L is the length of the impermeable core, N is the number of capsules, and V is the matrix volume. Each capsule is surrounded by a shell with thickness h (Fig. 4) which models the polymer regions whose permeability increases due to the interaction with the CNT surface. When the shells are overlapped, the capsules are organized into a cluster. When the cluster dimensions exceed the matrix volume, a *percolation cluster* is formed. For each fixed concentration of capsules, 1000 simulations were conducted, and the average volume occupied by highly permeable polymer regions is calculated as:

$$x_\infty = \left(\frac{4\pi}{3} \cdot (R^3 - R_0^3) + \pi \cdot (R^2 - R_0^2) \cdot L \right) \cdot \frac{N_\infty}{V} \quad (4)$$

Here, N_∞ is the number of capsules in the percolation cluster, x_∞ is proportional to the volume of highly permeable polymer regions which control the membrane permeability. Figure 5 shows x_∞ plotted against the volume concentration of the capsules with different diameters.

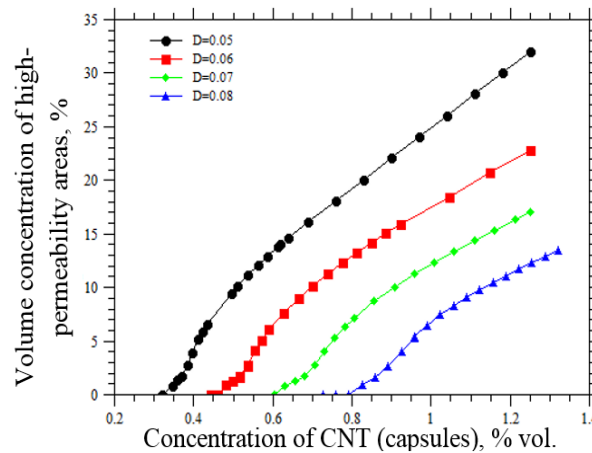


Figure 5. Volume concentration of the highly permeable regions in the matrix containing different amount of capsules

As follows from Fig. 5, for the capsules with the diameter of 0.05 which corresponds to the individual nanotubes, a percolation cluster is formed when the volume concentration of capsules increases from 0.3 to 0.35%; however, in this case, the content of the highly permeable regions is nearly zero. As the volume concentration of capsules increases from 0.35 to 0.5%, the concentration of highly permeable regions increases and χ_∞ becomes as high as 15% (with respect to the volume of the matrix). When the concentration of capsules is further increased, the concentration of the highly permeable regions linearly increases. Similar changes in the dimensions of the percolation regions are also observed for the bigger capsules but, as the capsules become bigger, the concentration of capsules at which the percolation cluster is formed increases.

Figure 6 shows the permeability coefficients of the PVTMS/CNT membranes calculated after the substitution of χ_∞ to Eq. (4). In these calculations, we assume that there is no gas transfer through inner CNT channels, and the increase in gas permeability is solely provided by gas transport through the highly permeable layer of the modified polymer near the CNT surface. This assumption is valid only for the permeability coefficient P_∞ but has no effect on the threshold concentrations corresponding to the formation of the percolation cluster and related changes in permeability.

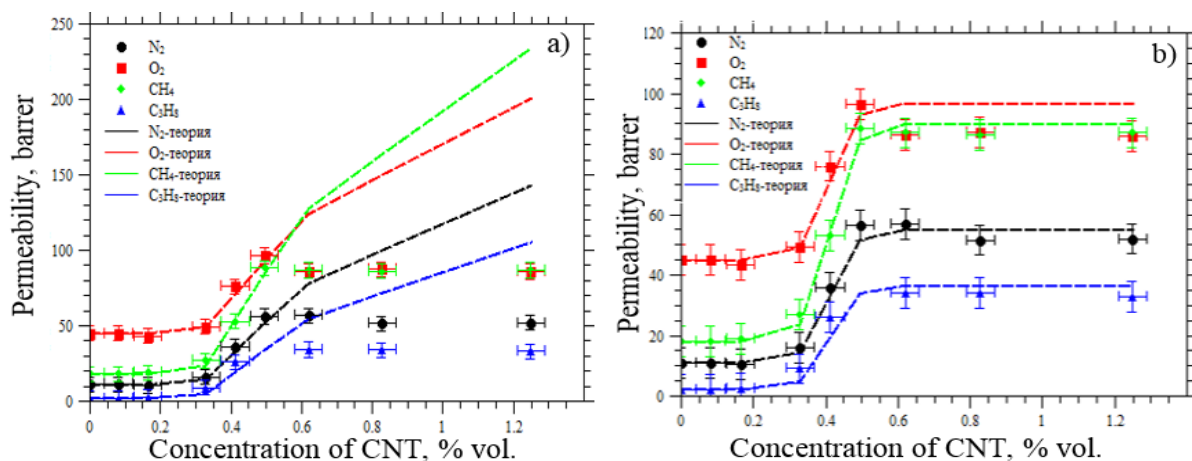


Figure 6. Gas permeability for reference (model) gases through the PVTMS/CNT membranes for (a) individual nanotubes and (b) with the account for agglomeration

Figure 6 shows the permeability coefficients of the PVTMS/CNT membranes calculated after the substitution of χ_∞ to Eq. (4). In these calculations, we assume that there is no gas transfer through

inner CNT channels, and the increase in gas permeability is solely provided by gas transport through the highly permeable layer of the modified polymer near the CNT surface. This assumption is valid only for the permeability coefficient P_{∞} but has no effect on the threshold concentrations corresponding to the formation of the percolation cluster and related changes in permeability. The calculated P_{∞} values (which are constant for each gas over the CNT concentration interval) are listed in Table 1.

Table 1. Permeability of PVTMS and percolation cluster

| Gas | Permeability of PVTMS, barrer | Permeability of the percolation cluster, barrer |
|-------------------------------|----------------------------------|--|
| N ₂ | 11 | 429 |
| O ₂ | 44 | 507 |
| CH ₄ | 18 | 702 |
| C ₃ H ₈ | 2 | 335 |

As follows from Fig. 6a, the calculated permeability coefficients well agree with the experimental values when the concentration of nanotubes in the matrix is below 0.5%. The development of the percolation structure and threshold changes in permeability are observed when the volume concentration of nanotubes varies from 0.3 to 0.4%. When the volume concentration of CNTs is above 0.5% (1.2wt %), the calculated permeability coefficients appear to be appreciably higher as compared with the experimental values. This disagreement can be explained by different parameters of the percolation cluster due to the agglomeration of nanotubes with increasing their content in the membrane. As follows from Fig. 6, when the average diameter of capsules increases due to the coalescence and agglomeration of nanotubes, the volume fraction of highly permeable regions at the same concentration of the capsules in the matrix decreases. For example, if the concentration of the capsules in the matrix is 0.008, as the diameter of the capsules increases from 0.05 to 0.06 (by 20%), the volume fraction of the percolation cluster decreases from 0.077 to 0.067 (by 13%); when the diameter is equal to 0.8, x_{∞} approaches zero! Figure 7b shows the permeability coefficients calculated according to Eq. (4) with the account for agglomeration plotted against volume fraction of CNTs. These calculations show that, when the CNT volume concentration varies from 0.5% to 1.2%, the permeability coefficient is constant only if the diameter of the capsules linearly increases from 0.05 to 0.09 units, which corresponds to the formation of the CNT agglomerates with an average size of about 100 nm.

Nonlinear changes in permeability lead to marked changes in the ideal selectivity of the membranes with increasing concentration of CNTs (Fig. 8). For example, separation factor $\alpha(\text{O}_2/\text{N}_2)$ decreases from 4 down to 1.7 as the CNT concentration increases from 0.5 to 1.2 wt %; at higher concentrations, $\alpha(\text{O}_2/\text{N}_2)$ remains unchanged. On the other hand, $\alpha(\text{CH}_4/\text{N}_2) = 1.7$ for all CNT concentrations within the margin of error; in the percolation interval, $\alpha(\text{C}_3\text{H}_8/\text{N}_2)$ increases from 0.2 to 0.6 and this value remains unchanged when the CNT concentration is higher than 1.2 wt %. The above changes in the separation factors prove the molecular mechanism of gas transport in the percolation membrane structure.

Conclusions

This work addresses the experimental study of gas permeability through the mixed matrix PVTMS/CNT membranes when the CNT concentration is higher than the percolation threshold. According to the experimental results, as the CNT concentration varies from 0.4% to 1.2 wt %, permeability of the CNT-containing membranes markedly increases: 5 times for nitrogen, 2 times for oxygen, 4 times for methane, and 15 for propane. However, further increase in the CNT content does not lead to any changes in permeability. This behavior (effect, phenomenon) was explained by the

numerical simulation of a percolation cluster composed of capsules in the 3D matrix with the dimensions equivalent to nanotubes and membranes. Changes in the volume of the percolation cluster are shown to control the threshold changes in the permeability of the mixed matrix membranes upon the percolation transition. Experimentally observed changes in the membrane permeability at high CNT concentrations can be explained with the account for the agglomeration of nanotubes (capsules) and related changes in the dimensions of the percolation cluster.

This work shows that, for the mixed matrix CNT-containing membranes, there exists the concentration interval where gas permeability dramatically increases. At high (excessive) concentrations of CNTs, due to agglomeration of nanotubes and deterioration of the percolation structure, further increase in the CNT concentration does not provide any improvement in the membrane performance.

References

- [1] Noble R 2011 *J. Membr. Sci.* **378** 393
- [2] Kim S, Pechar T and Marand E 2006 *Desalination* **192** 330
- [3] Andradý A, Merkel T and Toy L 2004 *Macromolecules* **37** 4329
- [4] Gomes D, Nunes S and Peinemann K 2005 *J. Membr. Sci.* **246** 13
- [5] Ma H and Gao X 2008 *Polymer* **49** 4230
- [6] Ahmad A, Jawad Z, Low S, Zein S 2012 *J. Membr. Sci.* **451** 55
- [7] Ge L, Zhu H and Rudolph V 2011 *Sep. Pur. Technol.* **78** 76
- [8] Khan M, Filiz V, Bengtson G, Shishatskiy S, Rahman M, Lillepaerg J and Abetz V 2013 *J. Membr. Sci.* **436** 109
- [9] Ismail A, Rahim N, Mustafa A, Matsuura T, Ng B, Abdullah S and Hashemifard S 2011 *Sep. Purif. Technol.* **80** 20
- [10] Jae-Hyun C, Jonggeon J, Woo-Nyon K and Ho-Sang C 2009 *J. Appl. Polym. Sci.* **111** 2186
- [11] Grekhov A, Eremin Yu, Dibrov G and Volkov V 2013 *Petrol. Chem.* **53** 549
- [12] Hung N, Anoshkin I, Dementjev A, Katorov D and Rakov E 2008 *Inorg. Mater.* **44** 270
- [13] Yampolskii Yu and Volkov V 1991 *J. Membr. Sci.* **64** 191
- [14] International Standard ISO13321
- [15] Barrett E, Joyner L and Halenda P 1951 *J. Am. Chem. Soc.* **73** 373
- [16] Brunauer S, Emmett P and Teller E 1938 *J. Am. Chem. Soc.* **60** 309
- [17] Grekhov A, Belogorlov A, Yushkin A and Volkov A 2012 *J. Membr. Sci.* **390-391** 160
- [18] Matsumoto M. M 1998 *ACM Trans. Mod. Comp. Simul.* **8** 3
- [19] Hoshen, J and Kopelman R 1976 *Phys. Rev. B* **14** 3438
- [20] Rubin, F. 1974 *IEEE Trans. Comp.* **23** 907
- [21] Lee M. 2007 *Phys. Rev. E* **76** 027702
- [22] Yampolsky Yu, Starannikova L and Belov N 2014 *Membr. Membr technol.* **4** 231
- [23] Winberg P, Sitter K, Dotremont C, Mullens S, Vankelecom I and Maurer F 2005 *Macromol.* **38** 3776
- [24] Merkel T, Freeman B, Spontak R, He Z, Pinnau I, Meakin P and Hill A 2002 *Science* **296** 519
- [25] Zhong J, Wen W and Jones A 2003 *Macromol.* **36** 6430
- [26] Matteucci S, Kusuma V, Sanders D, Swinnea S and Freeman B 2008 *J. Membr. Sci.* **307** 196
- [27] Kong Y, Du H, Yang J, Shi D, Wang Y, Zhang Y and Xin W 2002 *Desalination* **146** 49
- [28] Ahmad J and Hagg M 2013 *J. Membr. Sci.* **445** 200
- [29] Moniruzzaman M and Winey K 2006 *Macromolecules* **39** 5194
- [30] Shirazi Y, Tofighy M and Mohammadi T 2001 *J. Membr. Sci.* **378** 551
- [31] Cong H, Zhang J, Radosz M and Shen Y 2007 *J. Membr. Sci.* **294** 178
- [32] Kim S, Chen L, Johnson J and Marand E 2007 *J. Membr. Sci.* **294** 147